Measurement-End Dependence of Counter-Propagating Crosstalk in Spooled Multi-Core Fiber

Yuto Kobayashi, Shin Sato, Yuki Kawaguchi and Takemi Hasegawa
Optical Communications Laboratory, Sumitomo Electric Industries, Ltd., 1, Taya-cho, Sakae-ku 244-8588 Yokohama, Japan.
kobayashi-yuto@sei.co.jp

Abstract: We clarified theoretically and experimentally that the counter-propagating crosstalk in spooled multi-core fiber changes depending on the end for measurement, which indicates the need for management of conditions in measuring the counter-propagating crosstalk.

1. Background

Multi-core fiber (MCF) is a strong candidate to overcome the theoretical capacity limit of transmission in current single-core fiber. On the transmission in MCF, the crosstalk (XT) adds noise to signal. To reduce it, the counter-propagating scheme is a promising way [1]. Therefore, counter-propagating XT is an important property for the transmission system using MCF. Counter-propagating XT of MCF is usually measured with fiber spool before cabling and constructing transmission system, in order to guarantee its ability of transmission. However, the bending radius of spooled fiber changes along the fiber length and it causes longitudinal dependence of the coupling coefficient of the fiber [2].

In this paper, we calculated and measured co-propagating and counter-propagating XT when the coupling coefficient has fiber longitudinal dependence. We quantitatively clarified that the counter-propagating XT changes depending on which end the MCF is measured from and confirmed it with measurement. These results indicate that conditions such as spool radius, fiber length and measurement ends should be managed when defining the measurement of counter-propagating XT of spooled MCF.

2. Theory of XT with longitudinally varying coupling coefficient

We assume a 2-core MCF where the longitudinal development of the power in each core is described as

$$\frac{d}{dz}\begin{pmatrix}P_1\\P_2\end{pmatrix} = H(z)\begin{pmatrix}P_1\\P_2\end{pmatrix}, \qquad H(z) = \begin{pmatrix}-\alpha - h(z) & h(z)\\ h(z) & -\alpha - h(z)\end{pmatrix}, \qquad (1)$$

where z is the longitudinal position along the fiber, P_1 and P_2 are the powers of the fundamental modes in core 1 and 2 respectively, α is the attenuation in core 1 and 2 where attenuation is assumed to be constant along the fiber and between the cores, and $h(z)$ is the power coupling coefficient. Since $H(z)$ can be diagonalized by $\frac{1}{\sqrt{2}}\begin{pmatrix}1 & 1\\ 1 & -1\end{pmatrix}$, whose elements are constant for z, we obtain

$$\begin{pmatrix}P_1(z)\\P_2(z)\end{pmatrix} = \exp(-\alpha z)\exp\left(-\int_0^z h(z')dz'\right)\begin{pmatrix}\cosh\left(\int_0^z h(z')dz'\right) & \sinh\left(\int_0^z h(z')dz'\right)\\ \sinh\left(\int_0^z h(z')dz'\right) & -\cosh\left(\int_0^z h(z')dz'\right)\end{pmatrix}\begin{pmatrix}P_1(0)\\P_2(0)\end{pmatrix}. \qquad (2)$$

Because we can assume that $\int_0^z h(z')dz' \ll 1$ for uncoupled MCF, we can approximate $\exp\left(-\int_0^z h(z')dz'\right) \approx 1$, $\cosh\left(\int_0^z h(z')dz'\right) \approx 1$, and $\sinh\left(\int_0^z h(z')dz'\right) \approx \int_0^z h(z')dz'$ respectively. Since the co-propagating XT (XT_{co}) equals to $P_2(L)/P_1(L)$ when $P_1(0) = P_0$ and $P_2(0) = 0$ where L is the fiber length, from Eq. (2), we obtain

$$XT_{\mathrm{co}}(L) = \int_0^L h(z)dz. \qquad (3)$$

This equation shows that the co-propagating XT does not change depending on which end the fiber is measured from.

Counter-propagating XT (XT_{counter}) is defined as the ratio of the backward power of core 2 ($P_{\mathrm{back2}}(L)$) to the throughput power of core 1 ($P_1(L)$) when the power is input to core 1, that is, $XT_{\mathrm{counter}}(L) = P_{\mathrm{back2}}(L)/P_1(L)$. We note that $P_{\mathrm{back2}}(L)$ is defined as the power at $z = 0$ but it depends on the fiber length L, that is, $P_{\mathrm{back2}}(L)$ does not mean $z = L$ but means a function of L. Counter-propagating XT is mainly caused by Rayleigh backscattering when the splices and connectors have sufficiently low reflection [3]. Following the assumption in Ref. 3, we obtain

$$XT_{\mathrm{counter}}(L) = 2S\alpha_{\mathrm{R}}e^{\alpha L}\int_0^L \left(e^{-2\alpha z}XT_{\mathrm{co}}(z)\right)dz, \qquad (4)$$

where S is the proportion of the Rayleigh scattering component recaptured into a backward direction and α_R is the Rayleigh scattering loss coefficient. Finally, the difference between counter-propagating XT measured from the end A ($z = 0$) (XT_counterA) and that from the end B ($z = L$) (XT_counterB) can be calculated as below

$$XT_\mathrm{counterB} - XT_\mathrm{counterA} = \frac{2S\alpha_\mathrm{R}}{\alpha}\int_0^L h(z)\sinh\left(2\alpha\left(z-\frac{L}{2}\right)\right)dz. \quad (5)$$

This equation becomes zero when $h(z)$ is an even function at $z = L/2$, for example, when $h(z)$ is constant. It means that XT_counterA and XT_counterB are different in most case when $h(z)$ have dependence on fiber position z. In a spooled multi-core fiber, the coupling coefficient usually changes along length because the bending radius changes even when the fiber itself is uniformly fabricated. Consequently, Eq. (5) is usually not zero when the fiber under test is spooled.

3. Experiments and discussion

We evaluated the values of XT_co and XT_counter from each end with the direct power measurement. As shown in Fig. 1(a), we used wavelength scanning method with continuous-wave (CW) tunable light source (TLS). To avoid the difference of insertion loss of FIFO, we also measured XTs in case that the FIFOs were connected to the other end of fiber each other shown in Fig. 1(b) and these measured values were averaged in dB scale separately at each end. We also evaluated the fiber length dependence of XT_co using the multi-channel OTDR technique [4]. Fig. 1(c) shows the setup for measuring XT_co using a single channel OTDR with optical switches to realize the multi-channel OTDR technique with a single channel OTDR [5]. When the pulse signal from a laser diode (LD) is launched into Core 1 of the fiber under test for instance, the backscattered power from Cores 1 or 2 are detected corresponding to the selected path with the optical switches. Because the XT signal is very low, a relatively wide pulse width of 20 µsec was used for enhancing the signal to noise ratio. Tab. 1 summarizes the characteristics of the measurement sample. The sample was wounded on a spool with an inner diameter of 168 mm. We cut the sample into 60, 50, 40, 30, 20 and 10 km to measure the fiber length dependence of XT_co and XT_counter.

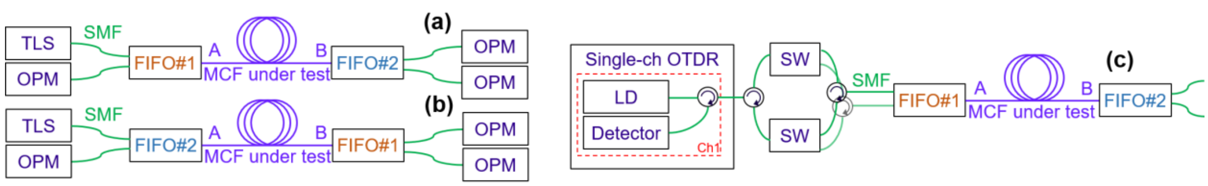

Fig. 1. Experimental setup for (a) direct power measurement using CW light source, (b) the same method as (a) with the FIFOs connected to the other end each other and (c) distributed XT measurement using single-channel OTDR. LD: laser diode, TLS: tunable light source, OPM: optical power meter and SW: optical switch.

Tab. 1. The properties of the sample at $\lambda = 1.55$ µm

Number of cores	α [dB/km]	A_eff [µm^2]	R_BS in dB for 1-ns pulse W	Cutoff wavelength [µm]	Fiber length [km]	FIFO XT [dB]
2	0.153	112	-84	1.47	68.3	-52.2

Fig. 2(a) shows the fiber position dependence of co-propagating XTs using distributed XT measurement technique. Fiber position dependences of co-propagating XTs are the same before and after the fiber under test cut into shorter. Fig. 2(b) shows derivation of co-propagating XT in Fig. 2(a) of $L = 68.3$ km. From Eq. (3), differentiated co-propagating XT equals to power coupling coefficient h. Therefore, the power coupling coefficient of the fiber under test is not constant for the fiber position nor even function at $z = L/2$, as shown in Fig. 2(b). It suggests that the counter-propagating XT measured from the end $z = 0$ km (end A) is different from that from the other end (end B).

We calculated the length dependence of co-propagating XT and counter-propagating XT with the distributed XT measurement results in the case the length of the fiber under test is $L = 68.3$ km using Eq. (3) and (4). The integrated power coupling coefficient from end B in Eq. (3) and (4) can be obtained from the formula

$$\int_0^z h_\mathrm{B}(z')dz' = \int_0^z h_\mathrm{A}(L-z')dz' = XT_\mathrm{coA}(L) - XT_\mathrm{coA}(L-z), \quad (6)$$

where $h_\mathrm{A}(z)$ and $h_\mathrm{B}(z)$ are the power coupling coefficients whose parameters z are defined as the position from A or B and XT_coA is the co-propagating XT measured from the end A. The calculated co and counter-propagating XTs from end A and B are shown in Fig. 2(c). Because the co-propagating XTs from end A and B are the same, we skipped to plot the co-propagating XT from end B. In Fig. 2(c), we also plotted the measured values of co and counter-propagating

XTs from end A and B using with the direct power measurement. The measured values of them agree with the calculated ones except XT_{counterB} in short fiber length. It is because the co-propagating XT measured with the OTDR technique has a dead-zone from 0 to ~3 km because the long pulse width of OTDR caused huge reflection at $z = 0$.

We also plotted the difference of co and counter-propagating XTs from end A and those from end B in dB scale in Fig. 2(d). $XT_{\mathrm{coB}} - XT_{\mathrm{coA}}$ is zero at each measured fiber lengths. On the other hand, $XT_{\mathrm{counterB}} - XT_{\mathrm{counterA}}$ is not zero at each measured fiber lengths. Therefore, we confirmed that counter-propagating XTs measured from end A and B are different when the coupling coefficient changes along the fiber length. We also plotted calculated values in Fig. 2(d), though, the calculated values of counter-propagating XT do not agree with the measured values in short length as we already mentioned. And it is also because subtracting small numbers from each other in dB scale causes large error even when the error value itself is small. To avoid it, we also calculated it with Eq. (4) as shown in Fig. 2(e). We note that the $XT_{\mathrm{counterB}} - XT_{\mathrm{counterA}}$ in Fig. 2(e) is subtracted in linear scale. The calculated values well agree with the measured values in this case. It is because the dead-zone in short length does not have a large effect to the integration in Eq. (5).

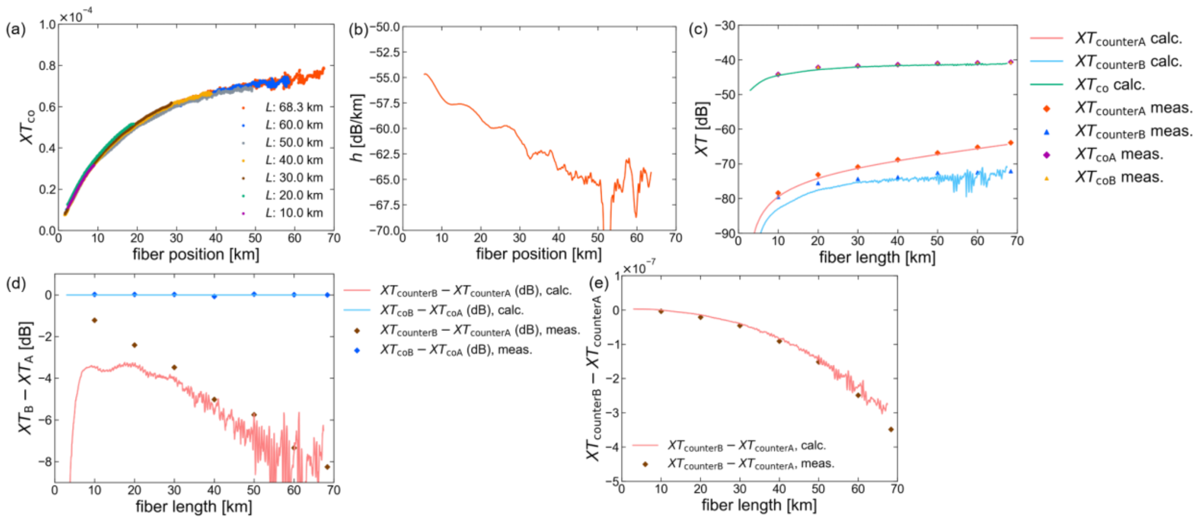

Fig. 2(a) fiber position dependence of co-propagating XTs using distributed XT measurement technique, (b) fiber position dependence of coupling coefficient calculated from the data shown in Fig. 2(a), (c) fiber length dependence of co and counter-propagating XT. The lines are calculated and the points are measured with the direct power measurement, (d) the difference of XTs measured from end A and B in dB scale, (e) the difference of counter-propagating XT measured from end A and B in linear scale.

4. Conclusions

We demonstrated that counter-propagating XT of spooled multi-core fiber depends on the measurement end because the bending radius and hence the power coupling coefficient of the measured fiber varies along the length. Consequently, when defining the measurement of counter-propagating XT, measurement conditions such as spool radius, fiber length and measurement ends should be managed.

5. References

[1] T. Hayashi *et al.*, in Proc. *Opt. Fiber Commun. Conf.*, 2021, Paper M1E.1.
[2] Y. Kobayashi *et al.*, in Proc. *OptoElectron. Commun. Conf./Photonics in Switching and Computing*, 2022, Paper TuC2-2.
[3] A. Sano *et al.*, *J. Light. Technol.*, vol. 32, no. 16, pp. 2771-2779, Aug. 2014.
[4] M. Nakazawa *et al.*, *Opt. Express*, vol. 20, no. 11, pp. 12530–12540, May 2012.
[5] Y. Kobayashi *et al.*, in Proc. *Asia Commun. and Photon. Conf.*, 2022, Paper 2563.